Recurrent triple-negative breast cancer from cysteine deprivation loses tumorigenicity via downregulation of the CST4 signaling

Xiaohu Tang (xiaohut@mtu.edu)
Michigan Technological University https://orcid.org/0000-0001-6367-4991
Tahiyat Alothaim
Michigan Technological University
Morgan Charbonneau
Michigan Technological University

Article

Keywords:

Posted Date: August 16th, 2022

DOI: https://doi.org/10.21203/rs.3.rs-1943456/v1

Recurrent triple-negative breast cancer from cysteine deprivation loses tumorigenicity via downregulation of the CST4 signaling

Tahiyat Alothaim[1], Morgan Charbonneau[1], Xiaohu Tang[1, 2]

[1] Department of Biological Sciences, Michigan Technological University, Houghton, Michigan, 49931

[2] Corresponding author: Xiaohu Tang;

E-mail: xiaohut@mtu.edu

Telephone: 906-487-3068

Conflict of Interest: The authors have declared no conflict of interests for this study.

Running title: Sustained cysteine deprivation suppresses tumorigenesis of mesenchymal-type triple-negative breast cancer

Abstract

Triple-negative breast cancer (TNBC) is an aggressive type of breast cancer with a high risk of recurrence following therapeutic treatments. Targeted cysteine therapy via inhibition of cysteine uptake by erastin effectively induces mesenchymal TNBC cells to ferroptosis. However, a small residual population of cancer cells exhibited the erastin-resistance and survived after the erastin treatment. This phenomenon is likely analogous to the event of tumor recurrence in patients after therapy. To characterize this resistance, we established the erastin-resistant/recurrent TNBC cell models *in vitro* by multi-cycles of erastin challenge. By an epigenetic compound library screen, the erastin-resistance be abolished by adjuvant epigenetic compounds. Intriguingly, the erastin-recurrent TNBC cells failed to grow in anchorage-independent conditions, implying a loss of tumorigenicity. By transcriptomic profiling analysis, the recurrent cells displayed many gene expression alterations and attenuated signaling processes, including K-Ras signaling. Three members of the cystatin gene family, including CST4, were significantly downregulated in recurrent cells. Knocking out of CST4 by CRISPR/Cas9 significantly suppressed the tumorigenic potential and K-Ras signaling. Our findings suggested that targeted cysteine therapy could be a valid treatment for mesenchymal TNBC with a low probability of tumor recurrence.

Introduction

Breast cancer is the first leading cause of cancer mortality in women globally, whereas triple-negative breast cancer (TNBC) is the most aggressive subtype with a high mortality rate. Surgery, chemotherapy, and emerging targeted therapies are therapeutic options for TNBC treatment [1-2]. Regardless of initial tumor responses to treatments, many tumors gain drug resistance and recurrence/relapse *in situ* from residual resistant tumor cells [2-3]. Recurrence is a major clinical manifestation of breast cancer and represents the major cause of cancer mortality. Particularly, TNBC frequently gains drug-resistance and distant recurrence within 3-5 years of surgery and therapeutic treatments [3-6].

Drug resistance is one of the major obstacles of cancer treatment. Generally, tumors acquire drug resistance by either intrinsic or acquired resistance mechanisms [7]. Intrinsic resistance involves innate molecular qualities of the tumor, including inter-tumor or intratumor heterogeneity [8]. On the other hand, the acquired resistance typically associates with gained molecular alterations in tumors during or after therapy, which is mediated by many different mechanisms, such as increasing drug efflux, alteration of drug metabolism, deregulation of cell signaling, changes in epigenetics and tumor microenvironment, *et al.* [9-14]. In TNBC, multidrug-resistant proteins are often upregulated to increase drug efflux. Mutations on cell death mediators and deregulated signaling have been reported to cause chemoresistance [15]. In addition, emerging evidences suggest that TNBC displays signatures of cancer stem cells at functional and molecular levels, which possesses tumor-initiating potential and self-renewal capacity, and increases the risks of drug resistance, metastasis, and recurrence [16-17].

Malignant tumor cells often exhibit altered cellular metabolisms, such as increased uptake of glucose or amino acids, which contribute to fast proliferation, tumorigenesis, and malignancy [18-20]. Targeting metabolic vulnerabilities in cancer is considered as a promising targeted therapeutic strategy. Since cysteine is required for the synthesis of glutathione (GSH), a major antioxidant against reactive oxidative species (ROS), cysteine deprivation leads to accumulation of lipid peroxidation and induces an iron-dependent ferroptosis [21-24]. Recently, targeted cysteine therapy by either inhibition of cysteine transporter (xCT) and GSH synthesis or inhibition of glutathione peroxidase 4 (GPX4) stands out as an effective option in treatment of a variety of cancers, including TNBC [25-32].

Breast cancer shows differentiated sensitivity to targeted cysteine therapy partially due to intertumoral heterogeneity. For example, the mesenchymal-type TNBC is highly sensitive to erastin, an inhibitor of xCT, while the epithelial-type TNBC is irresponsive [25, 33]. Epigenetic sensitizers have been identified to overcome the erastin-resistance in the epithelial TNBC [33]. Other mechanisms contributing to the erastin-resistance have been suggested in some cancers, such as activation of NRF2/CBS in ovarian cancer [34], degradation of VDAC2/3 melanoma [35], hypoxia, and extracellular cysteinyl glycine in glioblastoma [36], and deregulated cellular signaling in breast cancer [37-38]. It is necessary recapitulate molecular and cellular adaptations during or after targeted cysteine therapy and understand the underlying resistance mechanism.

In this study, we observed a small subpopulation of mesenchymal TNBC cells frequently escaping from cell death induced by cysteine deprivation. To characterize phenotypic and molecular changes, we established the erasin-resistant/recurrent TNBC

cell models *in-vitro*. We found that the recurrent TNBC cells lose the tumorigenic potential. By analyzing transcriptomic alterations in recurrent TNBC cells, we identified the downregulation of the CST4 signaling as one of the mechanisms to suppress tumorigenesis in TNBC.

Results

Establish *in vitro* erastin-resistant TNBC cell models by multiple-cycle of challenges

The mesenchymal TNBC cells are extremely sensitive to the xCT inhibitor erastin with prompt ferroptosis [25, 33]. However, about 1 ~ 5% of cell population were frequently observed resistant to erastin. Subsequently, these cells resumed growth and proliferation once the stress was removed. Such phenomena might reflect the facts of drug resistance and tumor recurrence in patients after therapy. To that end, we established the erastin-resistant/recurrent cell models *in vitro* to examine cellular characteristics and understand the underlying resistance mechanism. Two mesenchymal-type TNBC cells, MDA-MB-231 and BT549, were challenged under a series of 6 to 8 cycles of treatment and recovery from erastin to establish the erastin-resistant/recurrent (E^R) cells (**Fig. 1A**). Notably, both lines of erastin-resistant cells exhibit distinct morphologies with long stretched and neuron-like cell bodies with slower proliferation rates than their parental erastin-sensitive (E^S) cells (**Fig. 1B-C**). As expected, both MDA-MB-231 E^R and BT549 E^R cells were strongly resistant to erastin-induced ferroptosis when compared with their parental E^S cells (**Fig. 1D and S1A-B**). Importantly, MDA231 E^R and BT549 E^R cells were also significantly resistant to RSL3, a direct inhibitor of GPX4 (**Fig. 1E and S1C**). In consistent

with resistant phenotypes, immunoblotting analysis showed strong reductions of the death signaling (pho-p38) and DNA damage marker (pho-H2AX) in the E^R cells under erastin (**Fig. 1F**). In addition, the erastin-induced lipid peroxidation in the E^R cells was dramatically decreased when compared with the E^S cells (**Fig. S1D**).

Epigenetic compounds abolish the erastin-resistance in recurrent cells

It was reported that epigenetic compounds can render the non-mesenchymal TNBC cells sensitive to ferroptosis inducers [33]. Using a similar strategy of epigenetic compound library screening, three epigenetic compounds, targeting different epigenetic enzymes, were identified to potentially overcome the erastin-resistance in MDA-MB-231 E^R cells (**Fig. 2A**). Tubacin, an inhibitor of histone deacetylase HDAC6, synergized with erastin to induce an extensive ferroptosis in both MDA-MB-231 and BT549 E^R cells, but tubacin or erastin alone did not (**Fig. 2B-D** and **S2A).** In line with phenotypical responses, the death signaling and cell death markers were significantly activated in the E^R cells upon erastin plus tubacin (**Fig. 2E-F).** Similarly, two inhibitors for histone methyltransferases EZH2 (EPZ005687) or DOTL1 (SGC0946) abolished the erastin-resistance and induced significant cell death in MDA-MB-231 and BT549 E^R cells when combined with erastin (**Fig. S2B-C**). These results suggested that epigenetic inhibitors can serve as adjuvants to overcome the drug-resistance in the erastin-resistant/recurrent cells.

Erastin-resistant TNBC loses the potential of anchorage-independent growth

Intriguingly, we found that both MDA-MB-231 E^R and BT549 E^R hardly grew in an anchorage-independent condition, which indicated by a soft-agar colony formation assay (**Fig. 3A-B**). The colonies of E^R cells on soft-agar were significantly decreased in comparison with the E^S cells. Large colonies ($\geq$ 25 μm) were dramatically reduced in the E^R cells (**Fig. 3B).** Next, cell migration was more defective in the E^R cells than the E^S cells (**Fig. 3C)**. In addition, the E^R cells exhibited a distinct morphology with a relatively slow proliferation when growing in a three-dimensional (3D) low-attachment culture condition (**Fig. 3D**), in which the E^S cells displayed invadopodia-like structures, while the E^R cells mostly grew as spheroids. These data suggested that the E^R cells lose tumorigenic potentials in spite of their erastin-resistance.

Gene expressions and signaling are dramatically altered in recurrent E^R cells

To understand the underlying mechanism that contributes to loss of tumorigenicity in recurrent E^R cell models, the transcriptomic profiling was analyzed in MDA-MB-231 E^S and E^R cells. The gene cluster analysis indicated that numerous genes were altered in E^R cells in comparison with those in E^S cells, in which 156 genes were up-regulated, and 334 genes were down-regulated in E^R cells with at least 2-fold changes (**Fig. 4A**)**.** Gene set enrichment analysis (GSEA) revealed that the K-Ras, interferon, and hypoxia signaling pathways were significantly downregulated in E^R cells when compared with their parental counterparts (**Fig. 4B**). RT-qPCR analysis confirmed that gene expressions in the K-Ras and interferon pathways were significantly suppressed in E^R cells (**Fig. 4C and S3A**). The genes related to glutathione biosynthesis (GCLM and GCLC) and lipid peroxidation removal (GPX4) were increased in E^R cells (**Fig. S3B**). Interestingly, GSEA analysis

indicated that genesets associated with the neuronal cell type were enriched and highly expressed in E^R cells (**Fig. 4D**), which correlated with a neuron-like, multipolar, and stretched morphology in E^R cells (**Fig. 4E and S3C**). Taken together, these results indicated that the erastin-resistant/recurrent TNBC cells undergo many intrinsic changes in cellular signaling, metabolism, and structure to acquire the inability of tumorigenicity.

The cystatin genes are repressed in the E^R cells

Notably, we observed that the expressions of three cystatin family genes (*CST1, CST2*, and *CST4*) were significantly downregulated in both MDA-MB-231 and BT549 E^R cells (**Fig. 5A-B**), although the basal expression levels of cystatin genes in BT549 E^S cells were much lower than those in MDA-MB-231 cells. In agreement with the mRNA expression, the protein expression of CST4 was dramatically decreased in MDA-MB-231 E^R cells when compared with MDA-MB-231 E^S cells (**Fig. 5C**). It was reported that the expression of cystatin family genes contributes to poor prognosis, metastasis, and tumor relapse in a variety of cancers. Particularly, overexpression of CST1 or CST2 promotes tumor progression in gastric, breast, or colorectal cancer [39-43]. In TCGA breast invasive tumor samples, we found that the expression of CST4 is highly correlated with gene expressions of CST1 and CST2 (**Fig. 5D**).

CST4 regulates cellular signaling and tumorgenicity

The role of CST4 in either drug resistance or tumor progression, particularly in TNBC progression, is largely unknown. To that end, CST4 was knocked out in parental MDA-

MB-231 cells using two CST4-targeting CRISPR guide RNAs, and independent CST4-knockout (gCST4) cell clones were established (**Fig. 6A**). The gCST4 cells showed similar sensitivity to erastin as the wild-type cells (**Fig. S4A**), indicating that CST4 is not involved in the erastin-resistance. Intriguingly, the potential of gCST4 cells growing in the anchorage-independent condition was significantly reduced, in which the colonies were much smaller than their counterparts (**Fig. 6B and S4B**). Similar to the E^R cells, the genes involved in the K-Ras and interferon signaling were also significantly suppressed in the gCST4 cells (**Fig. 6C and S4C**). Interestingly, knockout of CST4 strongly repressed the transcription of *CST1* and *CST2*, even its own gene transcription (**Fig. 6D**), indicating that CST4 is an upstream signaling mediator of CST1 and CST2. Reciprocally, we overexpressed CST4 in BT549 cells, with a low basal level, to examined whether CST4 promotes tumorigenesis (**Fig. 6E**). Indeed, increased CST4 expression significantly enhanced the ability of cell growth in soft-agar (**Fig. 6F-G**). Cell migration was slightly increased when CST4 was overexpressed (**Fig. S4D**). Taken together, our data suggested that CST4 regulates cellular signaling and tumorgenicity, but not the erastin-resistance.

Discussion

Targeting metabolic vulnerability in tumors has been suggested as a promising targeted therapeutic strategy. We and others have shown that targeted cysteine therapy by blocking the cysteine-glutathione-GPX4 pathway induces ferroptosis in many types of cancers [22, 26, 44-46]. Particularly, mesenchymal-type triple negative breast cancer (TNBC) cells are extremely sensitive to ferroptosis inducers. However, a very small

subpopulation of cells remains survival or sustains proliferation after cysteine deprivation. Since tumor recurrence or relapse often occurs in triple-negative breast cancer (TNBC) within three years after chemotherapy or surgery [1, 3, 5], and the recurrent cells escaping from targeted cysteine therapy may pose potential risks for its clinic application, we established and characterized these erasrin-resistant/recurrent cells. The drug-resistant mechanisms, including Intra-tumoral heterogeneity and acquired resistance, are complex and vary with tumor types, genetics, and functional contexts [2, 5]. As we reported previously, HDAC6 inhibitors such as tubacin can be used as adjuvants to overcome the erastin-resistance in epithelial-type TNBC cells [33]. Similarly, the erastin-resistance in recurrent mesenchymal cells can be abolished by identified epigenetic inhibitors, such as histone deacetylase or methyltransferase inhibitors. Despite of morphological changes, the recurrent cells lack epithelial gene markers. The gene profiling and GSEA analysis showed a neuronal-like gene signature enriched in recurrent cells. This suggests that the underlying resistance mechanism in recurrent cells from mesenchymal-type TNBC may differ from that in epithelial-type TNBC.

Strikingly, the erasin-resistant/recurrent cells lose the ability of anchorage-independent growth, which may correlate with tumorigenic and metastatic potentials *in vivo*. This observation is further supported by the transcriptomic profiling analysis. GSEA analysis showed that the K-Ras, hypoxia, and interferon signaling gene signatures are impaired in recurrent cells, which are all known hallmarks of cancer. As well known, sustained K-Ras growth signaling and intra-tumoral hypoxia are important drive forces for breast cancer progression [47-49]. Recently, the interferon signaling in tumors has been

suggested as an inhibitory mechanism on immune destruction, which permits cancer cells to escape from immune clearance [50-53].

Notably, we observed a set of cystatin genes including *CST1, CST2*, and *CST4* are dramatically downregulated in the recurrent cells. Cystatins belong to a superfamily of cysteine protease inhibitors. The expression of CST1, and CST2 has been reported to be positively correlated with cancer progression [39-40]. High expression of CST1 in lung, gastric, pancreatic, colorectal, and breast cancer leads to poor prognosis, metastasis, and tumor relapse, while knockdown of CST1 suppresses tumor growth [54-56]. In addition, the epithelial and mesenchymal transition (EMT) and TGF- β signaling can be induced by CST2 in gastric cancer, which can promote metastasis and tumor progression [41]. CSTs have also been suggested as a prognostic biomarker for various cancers [57-59]. CST4, known as cystatin SA, was also founded highly expressed in gastric and colorectal cancer to promote cell proliferation, invasion, and metastasis [42, 60]. The role of CST4 in breast cancer, particularly in TNB[61]C, remains unclear. We observed that downregulation of CST4 associates with loss of tumorigenicity in recurrent cells. Knockout of CST4 mediated by CRISPR/Cas9 in parental erastin-sensitive cells recapitulates this phenomenon and suppresses tumorgenicity. Intriguingly, CST4 knockout causes dramatic downregulation of gene expression in the K-RAS and interferon signaling pathways. Furthermore, CST4 expression is positively correlated with the expression of CST1 and CST2 in TCGA breast tumor samples, and knockout of CST4 represses the transcription of *CST1* and *CST2*. All these observations suggest that CST4 acts as an upstream mediator of other cystatin genes and regulates multiple signaling pathways to promote tumorigenesis. Although similar downregulations were observed in another

recurrent cell model, these cystatins have relatively low basal expressions, suggesting that there are additional mechanisms to suppress tumorigenesis.

Taken together, our study suggests that targeted cysteine therapy via inhibition of the cysteine-GSH-GPX4 axis could be an effective strategy to treat mesenchymal TNBC with a low probability of tumor recurrence or relapse in patients. As an upstream mediator of multiple tumor-promoting signaling and its extracellular localization, CST4 could be a novel potential therapeutic target.

Materials and Methods

Cell culture and reagents

Breast cancer cells and 293T cells were all obtained from ATCC and cultured in DMEM supplemented with 10% fetal bovine serum (FBS) and 1% of antibiotics (Penicillin/Streptomycin) in a 95% humidified incubator at 37 ºC and 5% CO_2. To establish *in vitro* erastin-resistant/recurrent cell models, MDA-MB-321 and BT549 cells were treated with serial concentrations of erastin for 6~8 challenging cycles: Cells were treated with either 2 μM or 5 μM of erastin for seven days then recovered in fresh DMEM media without erastin; When reaching enough cell population, cells were subjected to next erastin-challenge until the cells were able to grow or showed no significant cell death under erastin. All compounds including erastin, RSL3, tubacin, EPZ005687, and SGC0946 were obtained from Cayman Chemicals (Ann Arbor, Michigan, US).

RNA extraction and quantitative RT-PCR

Total RNA was extracted from the cells by PureLink™ RNA kit (Invitrogen), 2 μg RNA were reverse transcribed by High-Capacity cDNA Reverse Transcription Kit (Thermo Fisher Scientific). The cDNA was subjected to quantitative PCR using SYBR Green PCR master mix (Applied Biosystems). The relative difference in mRNA expression was normalized with actin using the ΔΔCT method. All primers in this study were listed in Supplementary Table S1.

Gene expression profiling analysis

The gene expression profiles of MB-MDA-231 E^s and E^R cells in triplicate were analyzed by Clariom™ S Assay, human (ThermoFisher Scientific). The data were deposited in the GEO database (GSE202514). Probe intensities were normalized by RMAExpress and then subjected to hierarchical clustering analysis by Cluster 3.0. The pathway enrichment was analyzed by Gene Set Enrichment Analysis (GSEA) module using the G2 annotated-genesets with default criteria of 1000 permutations.

Immunoblot analysis

Cell pellets were lysed in RIPA buffer (Sigma) supplemented with the protease and phosphatase inhibitor cocktail (ThermoFisher Scientific). Protein concentrations were determined by the BCA protein assay. Equal amounts of protein were loaded in SDS-PAGE and transferred on the PVDF membrane for Western blot analysis. The signal was detected by the ECL plus Western blotting detection system (Bio-Rad) and visualized using LAS-4000 lumino image analyzer. The following antibodies were used in this study: PARP1 (9542S), phospho-p38 (4511S), phospho-H2AX (9718S), BNIP3 (44060S), β-actin (3700S), and β-Tubulin (86298S) were all obtained from Cell Signaling Technology. The CST4 antibody was obtained from GeneTex (GTX100690).

Lentiviral infection

Lentiviral particles were generated in 293T cells with lentiviral packaging plasmids using TransFectin™ Lipid Reagent (Bio-rad); the virus was collected from cell media after 48 hours of transfection. Cells were infected with indicated virus and followed by antibiotic selection. The plasmid pLX304-CST4 (Cat. #: HsCD00942127) was purchased from DNASU and the CRISPR/gRNA plasmids targeting CST4 were designed and purchased from VectorBuilder. pLX304-blasticidin and pLKO.1-puromycin vectors were used as controls.

Cell viability and epigenetic compound library screening

Cell viability and proliferation were measured by either trypan blue cell counting, CellTiter-Glo ATP assay kit (Promega), CytoTox-Fluor cytotoxicity assay kit (Promega), or Crystal Violet staining. The luminescent or fluorescent signals were measured by Synergy LX Multi-mode plate reader (BioTek). The epigenetic compound library screening was performed as described in the previous report [33].

Cell lipid peroxidation detection

Cells were stained with the Image-iT^{TM} Lipid Peroxidation Kit (Invitrogen) for 30 min and then incubated with a live cell imaging solution (ThermoFisher Scientific). Cell images under bright-light and fluorescence conditions were recorded by ZOE^{TM} Cell Imager (Bio-Rad).

Anchorage-independent cell growth and three-dimensional spheroid growth

Cells (3,000 cells/well) was resuspended in 2 mL DMEM plus 20% FBS with final 0.3% agar and layered on 0.6% basal agar. The feeding layer was added every 5 days.

After 20 days of incubation at 37°C, colonies were stained with crystal violet, colonies larger than 25 μm diameter were counted. Images were taken by camera and ZOE™ Cell Imager (Bio-Rad). To evaluate cell spheroid growth, 2000 cells per well were seeded into the ultra-low attachment 96-well plates (Corning). Cell morphology was monitored every two days and recorded by phase-contrast microscopy. Cell proliferation under three-dimension culture was examined by the CellTiter-Glo ATP assay kit at day 15.

Cell migration assay

Cells (5 x 10^5/well) were seeded in 6-well plates. When cells reached confluency, the wound was introduced by Pasteur pipette scratching; Floating cells were washed away by PBS, and then cells continued to grow in DMEM. Wound healing images were taken at indicated times using ZOE™ Cell Imager (Bio-Rad)..

Statistical analyses

The significance of differences between data groups was determined using a student *t* test. Statistical analysis was performed using GraphPad Prism 8.0 Software. A *p*-value < 0.05 was considered statistically significant. Data was presented in charts as mean ± standard deviation (SD).

Acknowledgments

This work was partially supported by the National Institute of Health (1R15CA246336-01) to X.T.

Reference

1 Bergin AR, Loi S. Triple-negative breast cancer: recent treatment advances. *F1000Research* 2019; 8.

2 Bianchini G, Balko JM, Mayer IA, Sanders ME, Gianni L. Triple-negative breast cancer: challenges and opportunities of a heterogeneous disease. *Nature reviews Clinical oncology* 2016; 13: 674-690.

3 Collignon J, Lousberg L, Schroeder H, Jerusalem GJBCT, Therapy. Triple-negative breast cancer: treatment challenges and solutions. *Breast Cancer: Targets Therapy* 2016; 8: 93.

4 Stewart RL, Updike KL, Factor RE, Henry NL, Boucher KM, Bernard PS *et al*. A multigene assay determines risk of recurrence in patients with triple-negative breast cancer. *Cancer research* 2019; 79: 3466-3478.

5 Yin L, Duan J-J, Bian X-W, Yu S-c. Triple-negative breast cancer molecular subtyping and treatment progress. *Breast Cancer Research* 2020; 22: 1-13.

6 Tang Y, Wang Y, Kiani MF, Wang B. Classification, treatment strategy, and associated drug resistance in breast cancer. *Clinical breast cancer* 2016; 16: 335-343.

7 Holohan C, Van Schaeybroeck S, Longley DB, Johnston PG. Cancer drug resistance: an evolving paradigm. *Nat Rev Cancer* 2013; 13: 714-726.

8 De Conti G, Dias MH, Bernards R. Fighting Drug Resistance through the Targeting of Drug-Tolerant Persister Cells. *Cancers (Basel)* 2021; 13.

9 De Angelis ML, Francescangeli F, Zeuner A. Breast cancer stem cells as drivers of tumor chemoresistance, dormancy and relapse: new challenges and therapeutic opportunities. *Cancers* 2019; 11: 1569.

10 Deepak K, Vempati R, Nagaraju GP, Dasari VR, Nagini S, Rao D *et al*. Tumor microenvironment: Challenges and opportunities in targeting metastasis of triple negative breast cancer. *Pharmacological research* 2020; 153: 104683.

11 Ensenyat-Mendez M, Llinàs-Arias P, Orozco JI, Íñiguez-Muñoz S, Salomon MP, Sesé B *et al*. Current Triple-Negative Breast Cancer Subtypes: Dissecting the Most Aggressive Form of Breast Cancer. *Frontiers in Oncology* 2021; 11.

12 Holohan C, Van Schaeybroeck S, Longley DB, Johnston PG. Cancer drug resistance: an evolving paradigm. *Nature Reviews Cancer* 2013; 13: 714-726.

13 Housman G, Byler S, Heerboth S, Lapinska K, Longacre M, Snyder N *et al*. Drug resistance in cancer: an overview. *Cancers* 2014; 6: 1769-1792.

14 Zhang T, Zhou H, Wang K, Wang X, Wang M, Zhao W *et al*. Role, molecular mechanism and the potential target of breast cancer stem cells in breast cancer development. *Biomedicine Pharmacotherapy* 2022; 147: 112616.

15 Nedeljkovic M, Damjanovic A. Mechanisms of Chemotherapy Resistance in Triple-Negative Breast Cancer-How We Can Rise to the Challenge. *Cells* 2019; 8.

16 Lee K-L, Kuo Y-C, Ho Y-S, Huang Y-H. Triple-negative breast cancer: current understanding and future therapeutic breakthrough targeting cancer stemness. *Cancers* 2019; 11: 1334.

17 Dent R, Trudeau M, Pritchard KI, Hanna WM, Kahn HK, Sawka CA *et al*. Triple-negative breast cancer: clinical features and patterns of recurrence. *Clin Cancer Res* 2007; 13: 4429-4434.

18 Hanahan D, Weinberg RA. Hallmarks of cancer: the next generation. *cell* 2011; 144: 646-674.

19 Hainaut P, Plymoth A. Targeting the hallmarks of cancer: towards a rational approach to next-generation cancer therapy. *Current opinion in oncology* 2013; 25: 50-51.

20 Pavlova NN, Zhu J, Thompson CB. The hallmarks of cancer metabolism: Still emerging. *Cell Metab* 2022; 34: 355-377.

21 Sun X, Wang M, Wang M, Yu X, Guo J, Sun T *et al*. Metabolic reprogramming in triple-negative breast cancer. *Frontiers in oncology* 2020; 10: 428.

22 Zhang C, Liu X, Jin S, Chen Y, Guo R. Ferroptosis in cancer therapy: a novel approach to reversing drug resistance. *Molecular Cancer* 2022; 21: 1-12.

23 Yang WS, Stockwell BR. Synthetic lethal screening identifies compounds activating iron-dependent, nonapoptotic cell death in oncogenic-RAS-harboring cancer cells. *Chem Biol* 2008; 15: 234-245.

24 Dixon SJ, Lemberg KM, Lamprecht MR, Skouta R, Zaitsev EM, Gleason CE *et al*. Ferroptosis: an iron-dependent form of nonapoptotic cell death. *Cell* 2012; 149: 1060-1072.

25 Tang X, Ding C-K, Wu J, Sjol J, Wardell S, Spasojevic I *et al*. Cystine addiction of triple-negative breast cancer associated with EMT augmented death signaling. *Oncogene* 2017; 36: 4235-4242.

26 Badgley MA, Kremer DM, Maurer HC, DelGiorno KE, Lee H-J, Purohit V *et al*. Cysteine depletion induces pancreatic tumor ferroptosis in mice. *Science* 2020; 368: 85-89.

27 Hao S, Yu J, He W, Huang Q, Zhao Y, Liang B *et al*. Cysteine dioxygenase 1 mediates erastin-induced ferroptosis in human gastric cancer cells. *Neoplasia* 2017; 19: 1022-1032.

28 Zhao Y, Li Y, Zhang R, Wang F, Wang T, Jiao Y. The role of erastin in ferroptosis and its prospects in cancer therapy. *OncoTargets therapy* 2020; 13: 5429.

29 Tang X, Wu J, Ding C-K, Lu M, Keenan MM, Lin C-C *et al*. Cystine deprivation triggers programmed necrosis in VHL-deficient renal cell carcinomas. *Cancer research* 2016; 76: 1892-1903.

30 Yu Y, Xie Y, Cao L, Yang L, Yang M, Lotze MT *et al*. The ferroptosis inducer erastin enhances sensitivity of acute myeloid leukemia cells to chemotherapeutic agents. *Molecular cellular oncology* 2015; 2: e1054549.

31 Lei G, Zhang Y, Koppula P, Liu X, Zhang J, Lin SH *et al*. The role of ferroptosis in ionizing radiation-induced cell death and tumor suppression. *Cell Res* 2020; 30: 146-162.

32 Hangauer MJ, Viswanathan VS, Ryan MJ, Bole D, Eaton JK, Matov A *et al*. Drug-tolerant persister cancer cells are vulnerable to GPX4 inhibition. *Nature* 2017; 551: 247-250.

33 Alothaim T, Charbonneau M, Tang X. HDAC6 inhibitors sensitize non-mesenchymal triple-negative breast cancer cells to cysteine deprivation. *Scientific Reports* 2021; 11: 1-11.

34 Liu N, Lin X, Huang C. Activation of the reverse transsulfuration pathway through NRF2/CBS confers erastin-induced ferroptosis resistance. *British journal of cancer* 2020; 122: 279-292.

35 Yang Y, Luo M, Zhang K, Zhang J, Gao T, Connell DO *et al*. Nedd4 ubiquitylates VDAC2/3 to suppress erastin-induced ferroptosis in melanoma. *Nature communications* 2020; 11: 1-14.

36 Hayashima K, Katoh H. Expression of gamma-glutamyltransferase 1 in glioblastoma cells confers resistance to cystine deprivation-induced ferroptosis. *Journal of Biological Chemistry* 2022: 101703.

37 Lin CC, Yang WH, Lin YT, Tang X, Chen PH, Ding CC *et al*. DDR2 upregulation confers ferroptosis susceptibility of recurrent breast tumors through the Hippo pathway. *Oncogene* 2021; 40: 2018-2034.

38 Lin CC, Mabe NW, Lin YT, Yang WH, Tang X, Hong L *et al*. RIPK3 upregulation confers robust proliferation and collateral cystine-dependence on breast cancer recurrence. *Cell Death Differ* 2020; 27: 2234-2247.

39 Chen S, Liu Y, Zhang K, Chen L. CST1 promoted gastric cancer migration and invasion through activating Wnt pathway. *Cancer Management Research* 2021; 13: 1901.

40 Dai D-n, Li Y, Chen B, Du Y, Li S-b, Lu S-x *et al*. Elevated expression of CST1 promotes breast cancer progression and predicts a poor prognosis. *Journal of Molecular Medicine* 2017; 95: 873-886.

41 Zhang W, Wang Y, Tan D, Xing C. Cystatin 2 leads to a worse prognosis in patients with gastric cancer. *Journal of Biological Regulators Homeostatic Agents* 2020; 34.

42 Zhang YQ, Zhang JJ, Song HJ, Li DW. Overexpression of CST4 promotes gastric cancer aggressiveness by activating the ELFN2 signaling pathway. *American journal of cancer research* 2017; 7: 2290.

43 Jiang J, Liu H-L, Tao L, Lin X-Y, Yang Y-D, Tan S-W *et al*. Let-7d inhibits colorectal cancer cell proliferation through the CST1/p65 pathway. *International Journal of Oncology* 2018; 53: 781-790.

44 Tang X, Ding CK, Wu J, Sjol J, Wardell S, Spasojevic I *et al*. Cystine addiction of triple-negative breast cancer associated with EMT augmented death signaling. *Oncogene* 2017; 36: 4235-4242.

45 Bebber CM, Thomas ES, Stroh J, Chen Z, Androulidaki A, Schmitt A *et al*. Ferroptosis response segregates small cell lung cancer (SCLC) neuroendocrine subtypes. *Nature Communications* 2021; 12: 2048.

46 Tang X, Wu J, Ding CK, Lu M, Keenan MM, Lin CC *et al*. Cystine Deprivation Triggers Programmed Necrosis in VHL-Deficient Renal Cell Carcinomas. *Cancer Res* 2016; 76: 1892-1903.

47 de Heer EC, Jalving M, Harris AL. HIFs, angiogenesis, and metabolism: elusive enemies in breast cancer. *J Clin Invest* 2020; 130: 5074-5087.

48 Kim R-K, Suh Y, Yoo K-C, Cui Y-H, Kim H, Kim M-J *et al*. Activation of KRAS promotes the mesenchymal features of basal-type breast cancer. *Experimental molecular medicine* 2015; 47: e137-e137.

49 Fultang N, Chakraborty M, Peethambaran B. Regulation of cancer stem cells in triple negative breast cancer. *Cancer Drug Resist* 2021; 4: 321-342.

50 Provance OK, Lewis-Wambi J. Deciphering the role of interferon alpha signaling and microenvironment crosstalk in inflammatory breast cancer. *Breast Cancer Res* 2019; 21: 59.

51 Boukhaled GM, Harding S, Brooks DG. Opposing Roles of Type I Interferons in Cancer Immunity. *Annu Rev Pathol* 2021; 16: 167-198.

52 Benci JL, Johnson LR, Choa R, Xu Y, Qiu J, Zhou Z *et al*. Opposing Functions of Interferon Coordinate Adaptive and Innate Immune Responses to Cancer Immune Checkpoint Blockade. *Cell* 2019; 178: 933-948 e914.

53 Wang L, Zhao Y, Liu Y, Akiyama K, Chen C, Qu C *et al*. IFN-γ and TNF-α synergistically induce mesenchymal stem cell impairment and tumorigenesis via NFκB signaling. *Stem cells* 2013; 31: 1383-1395.

54 Kim J-T, Lee S-J, Kang M, Park J, Kim BY, Yoon D *et al*. Cystatin SN neutralizes the inhibitory effect of cystatin C on cathepsin B activity. *Cell death disease* 2013; 4: e974-e974.

55 Liu Y, Ma H, Wang Y, Du X, Yao J. Cystatin SN affects cell proliferation by regulating the ERα/PI3K/AKT/ERα loopback pathway in breast cancer. *OncoTargets therapy* 2019; 12: 11359.

56 Oh S-S, Park S, Lee K-W, Madhi H, Park SG, Lee HG *et al*. Extracellular cystatin SN and cathepsin B prevent cellular senescence by inhibiting abnormal glycogen accumulation. *Cell death disease* 2017; 8: e2729-e2729.

57 Xie Q, Liu L, Chen X, Cheng Y, Li J, Zhang X *et al*. Identification of Cysteine Protease Inhibitor CST2 as a Potential Biomarker for Colorectal Cancer. *Journal of Cancer* 2021; 12: 5144.

58 Lai Y, Wang Y, Wu Y, Wu M, Xing S, Xie Y *et al*. Identification and Validation of Serum CST1 as a Diagnostic Marker for Differentiating Early-Stage Non-Small Cell Lung Cancer from Pulmonary Benign Nodules. *Cancer Control* 2022; 29: 10732748221104661.

59 Cai L, Tu M, Yin X, Zhang S, Zhuang W, Xia Y *et al*. Combination of serum CST4 and DR-70 contributes to early diagnosis of colorectal cancer. *Clin Chim Acta* 2022; 531: 318-324.

60 Shi D, Zhou Z, Zhang S. miRNA-6715-5p Inhibits Cellular Proliferation and Invasion in Colorectal Cancer by Directly Targeting CST4. *Journal of oncology* 2021; 2021.

61 Wang S, Wang C, Liu O, Hu Y, Li X, Lin B. Prognostic value of immune-related cells and genes in the tumor microenvironment of ovarian cancer, especially CST4. *Life Sci* 2021; 277: 119461.

Figure legends

Figure 1. Establishment of *in vitro* erastin-resistant cells from mesenchymal TNBC

(**A**) Scheme of establishing recurrent MDA-MB-231 and BT549 cells from multiple cycles of the erastin treatment.

(**B**) Cell morphology of MDA-MB-231 and BT549 parental cells (E^S) and erastin-resistant cells (E^R). Scale bar = 100 μm.

(**C**) Cell growth curves of MDA-MB-231 and BT549 E^S vs. E^R cells (n=3; *, $p < 0.001$).

(**D, E**) Relative cell survival of MDA-MB-231 and BT549 E^S vs. E^R cells was measured by CellTiter-Glo ATP assay under either control, 5 μM erastin (**D**), or 1 μM RSL3 (**E**) treatments for 24 hrs (n=3; **, $p < 0.001$).

(**F**) Immunoblotting analysis of pho-p38, pho-H2AX in E^S and E^R cells under either control (Con) or 5 μM erastin (E) treatments for 18 hrs, β-actin was used for the loading normalization.

Figure 2. Epigenetic compound library screening identifies potent sensitizers for recurrent TNBC

(**A**) Cell viability was measured in MDA-MB-231 E^R cells treated with the epigenetic compound library under either the control (Con), or 5 μM erastin (E) conditions for 72 hrs.

(**B, C, D**) Relative cell survival of MDA-MB-231 E^R or BT549 E^R cells was assessed by either CellTiter-Glo assay or crystal violet staining under the control, 5 μM erastin (E), 5 μM tubacin (T), or erastin plus tubacin (E+T) treatments for 72 hrs (n=3; *, $p < 0.0001$).

(**E, F**) Immunoblotting of indicated markers in MB-MDA-231 E^R or BT549 E^R cells treated as (**B, C**).

Figure 3. Recurrent TNBC E^R cells lose tumorigenic potential

(**A**) Anchorage-independent growth of E^S vs. E^R cells in soft agar. Upper panel represents full-well images; lower panel shows cell colonies with magnification. (n=3, Scale bar= 25 μm).

(**B**) Quantification of colonies according to the size (n=3; *, $p<0.001$; **, $p<0.01$).

(**C**) Wound healing of E^S vs. E^R cells at 48 hrs.

(**D**) 3D-spheroid living images of MDA-MB-231 E^S vs. E^R at the day 7 (Scale bar = 100 μm); Cell viability was measured under the low attachment condition at the day 15 (n=3, **#**, $p<0.01$).

Figure 4. Gene transcriptomic profile is altered in recurrent TNBC

(**A**) Volcanic and heatmap view of gene expression changes in MDA-MB-231 E^S vs. E^R cells.

(**B**) Gene set enrichments by GSEA analysis in MDA-MB-231 E^S cells.

(**C**) RT-qPCR expression analysis of genes in the K-Ras signaling pathway in MDA-MB-231 E^S vs. E^R cells (n=4; *, $p<0.01$).

(**D**) Gene set enrichments by GSEA analysis in in MDA-MB-231 E^R cells.

(**E**) Cell morphology of MDA-MB-231 E^S and E^R cells at confluent stage.

Figure 5. Cystatin genes are downregulated in recurrent TNBC

(**A, B**) Relative expression of three cystatin-family genes in MDA-MB-231 and BT549 E^S vs. E^R cells (n=3; *, p<0.0001).

(**C**) CST4 protein expression in E^S vs. E^R cells.

(**D**) Correlation of gene expression between CST4 and either CST1 or CST2 in TCGA breast invasive carcinomas (p<0.001).

Figure 6. CST4 gene knockout suppresses the anchorage-independent growth

(**A**) Immunoblot analysis of CST4 protein expression in MDA-MB-231 vector (Vec) and CST4-knockout cell clones (gCST4).

(**B**) Anchorage-independent growth of MDA-MB-231 Vec and gCST4 cell clones (n=3, scale bar= 25 μm).

(**C**) RT-qPCR expression analysis of genes in the K-Ras signaling pathway in cells as (**B**) (n=4; $^\#$, p<0.0005).

(**D**) Relative expression of indicated cystatin genes in indicated cells as (**B**) (n=3; **, p<0.0001).

(**E**) Immunoblot analysis of CST4 protein expression in BT549 vector (Vec) and CST4-overexpressed cells.

(**F, G**) Anchorage-independent growth of BT549 Vec and CST4-overexpressed cells (n=3; *, p<0.01). Scale bar = 25 μm.

Figures

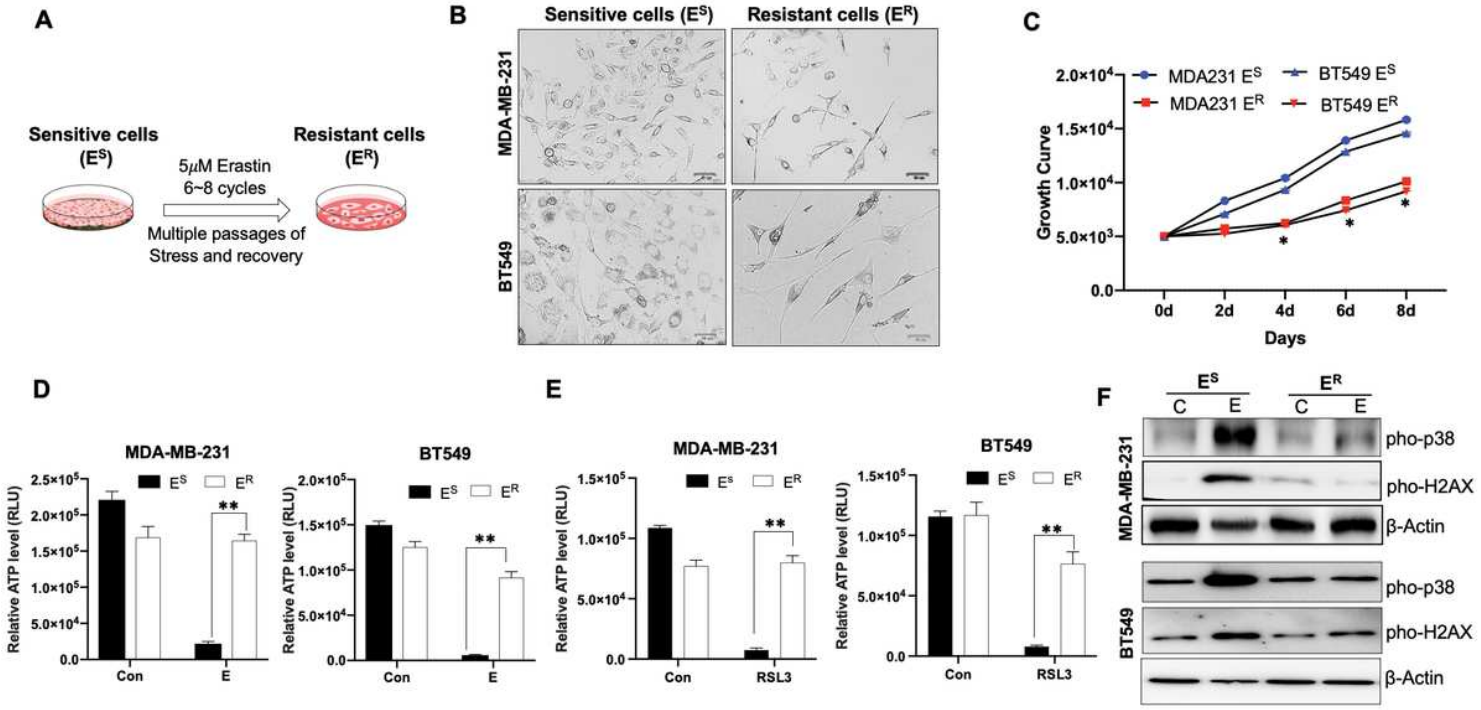

Figure 1

Establishment of in vitro erastin-resistant cells from mesenchymal TNBC (A) Scheme of establishing recurrent MDA-MB-231 and BT549 cells from multiple cycles of the erastin treatment. (B) Cell morphology of MDA-MB-231 and BT549 parental cells (ES) and erastin-resistant cells (ER). Scale bar = 100 μm. (C) Cell growth curves of MDA-MB-231 and BT549 ES vs. ER cells (n=3; *, p <0.001). (D, E) Relative cell survival of MDA-MB-231 and BT549 ES vs. ER cells was measured by CellTiter-Glo ATP assay under either control, 5 μM erastin (D), or 1 μM RSL3 (E) treatments for 24 hrs (n=3; **, p <0.001). (F) Immunoblotting analysis of pho-p38, pho-H2AX in ES and ER cells under either control (Con) or 5 μM erastin (E) treatments for 18 hrs, β-actin was used for the loading normalization.

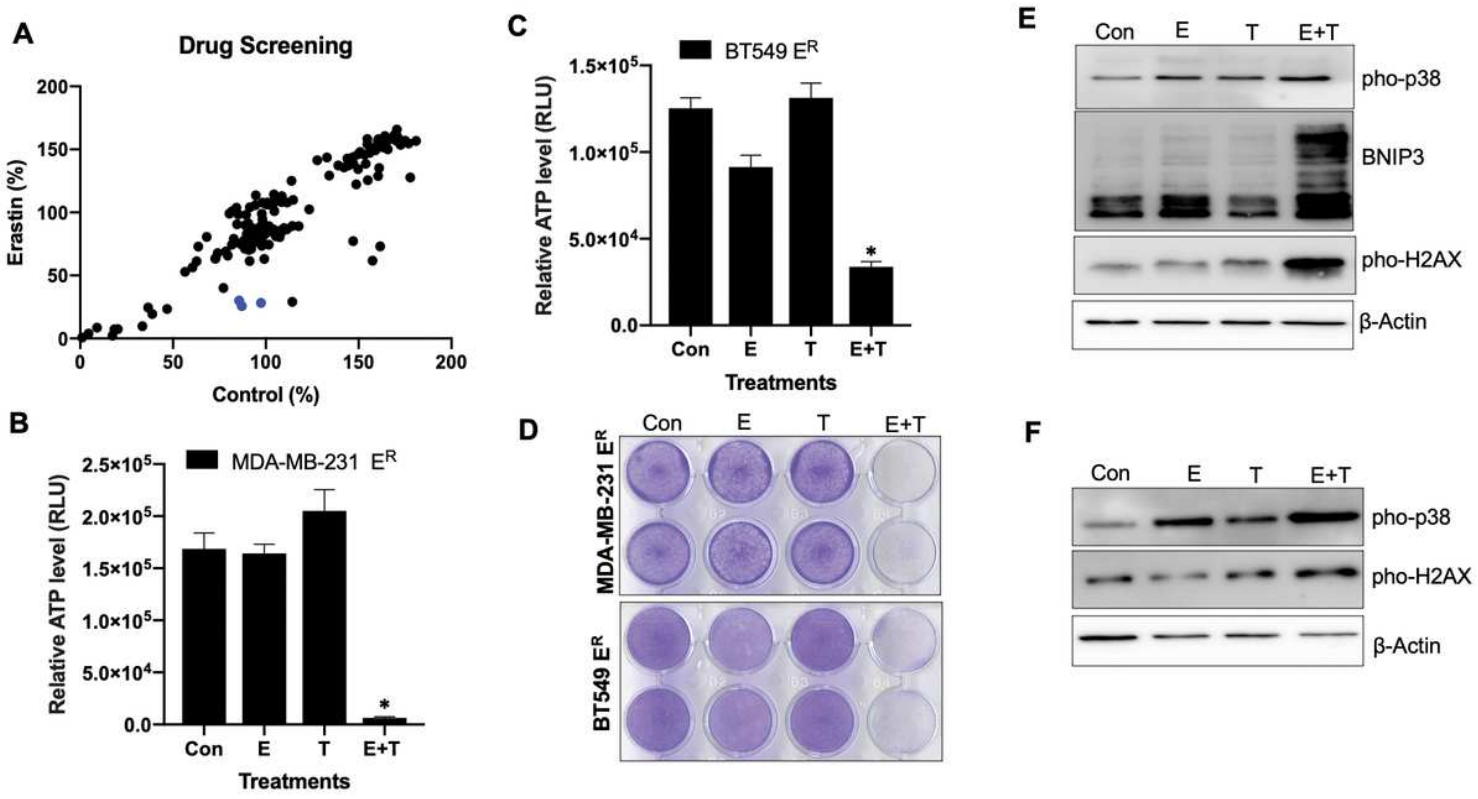

Figure 2

Epigenetic compound library screening identifies potent sensitizers for recurrent TNBC (A) Cell viability was measured in MDA-MB-231 ER cells treated with the epigenetic compound library under either the control (Con), or 5 μM erastin (E) conditions for 72 hrs. (B, C, D) Relative cell survival of MDA-MB-231 ER or BT549 ER cells was assessed by either CellTiter-Glo assay or crystal violet staining under the control, 5 μM erastin (E), 5 μM tubacin (T), or erastin plus tubacin (E+T) treatments for 72 hrs (n=3; *, p<0.0001). (E, F) Immunoblotting of indicated markers in MB-MDA-231 ER or BT549 ER cells treated as (B, C).

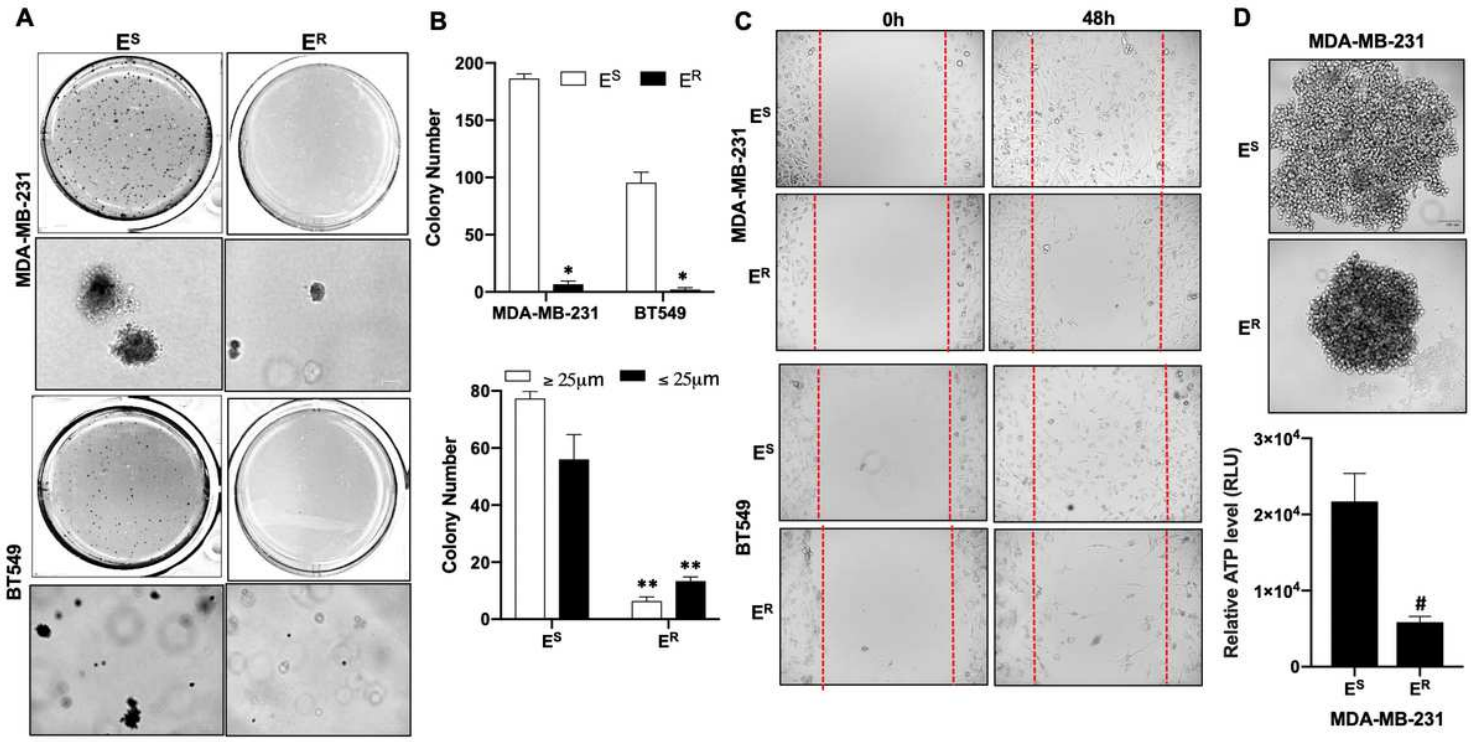

Figure 3

Recurrent TNBC ER cells lose tumorigenic potential (A) Anchorage-independent growth of ES vs. ER cells in soft agar. Upper panel represents full-well images; lower panel shows cell colonies with magnification. (n=3, Scale bar= 25 μm). (B) Quantification of colonies according to the size (n=3; *, $p<0.001$; **, $p<0.01$). (C) Wound healing of ES vs. ER cells at 48 hrs. (D) 3D-spheroid living images of MDA-MB-231 ES vs. ER at the day 7 (Scale bar = 100 μm); Cell viability was measured under the low attachment condition at the day 15 (n=3, #, $p<0.01$).

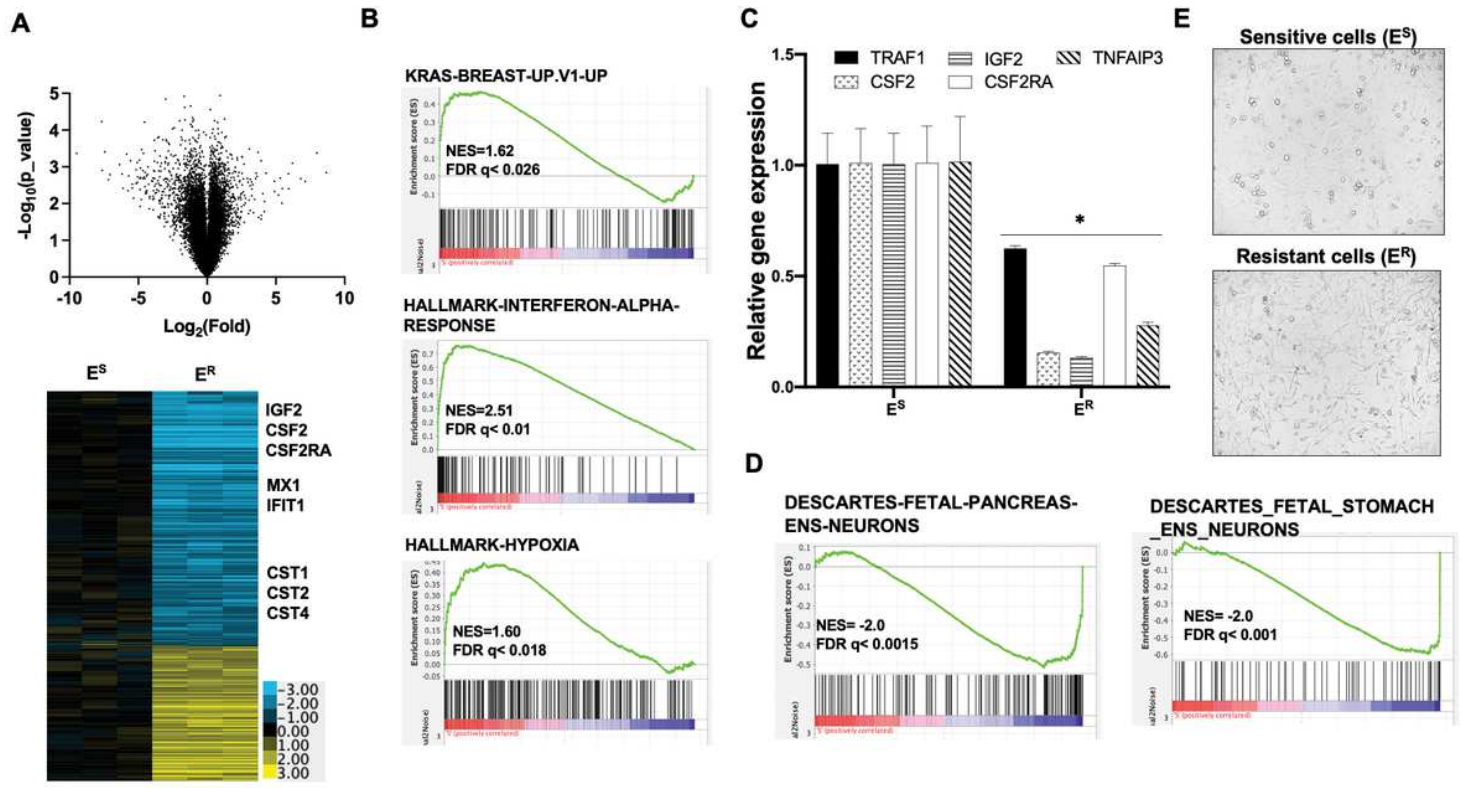

Figure 4

Gene transcriptomic profile is altered in recurrent TNBC (A) Volcanic and heatmap view of gene expression changes in MDA-MB-231 ES vs. ER cells. (B) Gene set enrichments by GSEA analysis in MDA-MB-231 ES cells. (C) RT-qPCR expression analysis of genes in the K-Ras signaling pathway in MDA-MB-231 ES vs. ER cells (n=4; *, p<0.01). (D) Gene set enrichments by GSEA analysis in in MDA-MB-231 ER cells. (E) Cell morphology of MDA-MB-231 ES and ER cells at confluent stage.

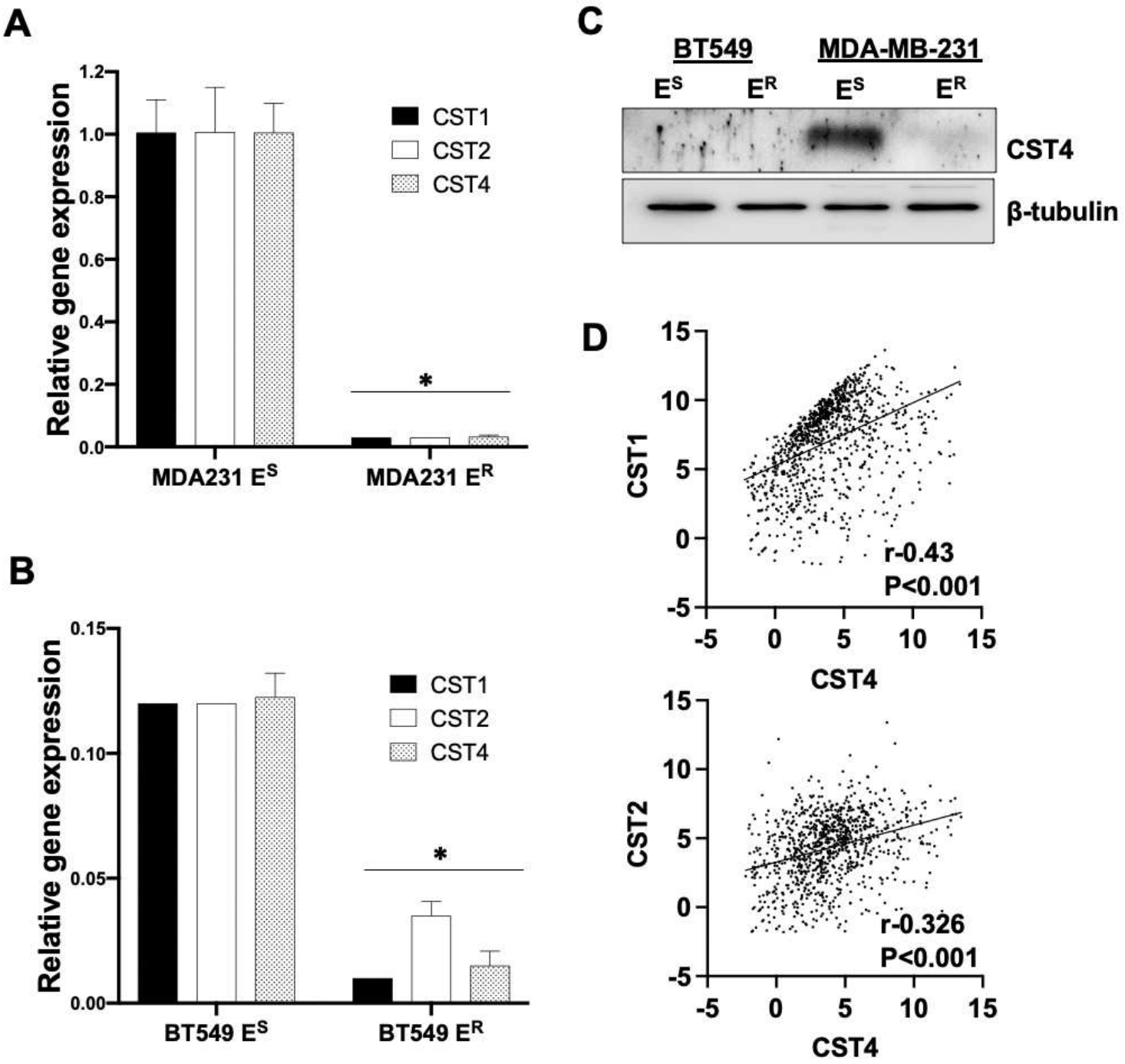

Figure 5

Cystatin genes are downregulated in recurrent TNBC (A, B) Relative expression of three cystatin-family genes in MDA-MB-231 and BT549 ES vs. ER cells (n=3; *, p<0.0001). (C) CST4 protein expression in ES vs. ER cells. (D) Correlation of gene expression between CST4 and either CST1 or CST2 in TCGA breast invasive carcinomas (p<0.001).

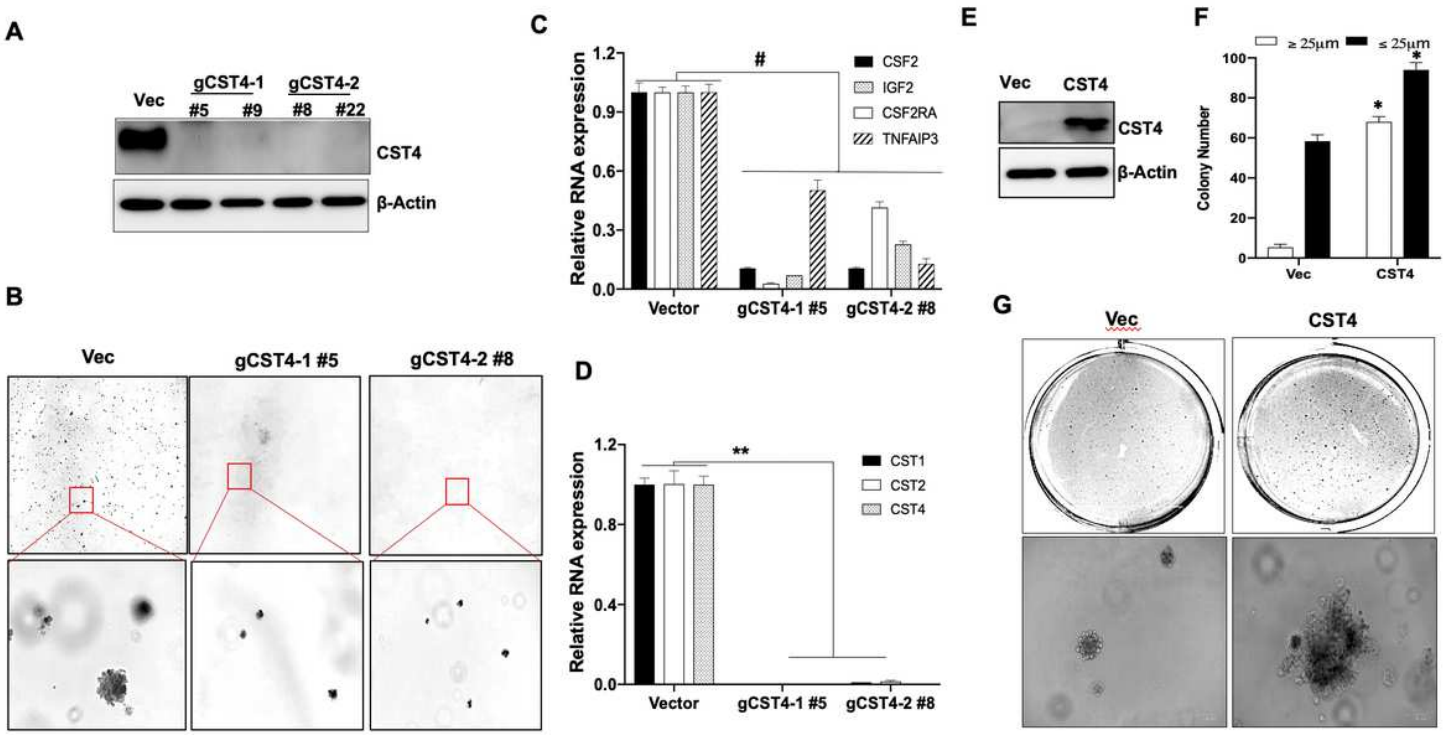

Figure 6

CST4 gene knockout suppresses the anchorage-independent growth (A) Immunoblot analysis of CST4 protein expression in MDA-MB-231 vector (Vec) and CST4-knockout cell clones (gCST4). (B) Anchorage-independent growth of MDA-MB-231 Vec and gCST4 cell clones (n=3, scale bar= 25 μm). (C) RT-qPCR expression analysis of genes in the K-Ras signaling pathway in cells as (B) (n=4; #, $p<0.0005$). (D) Relative expression of indicated cystatin genes in indicated cells as (B) (n=3; **, $p<0.0001$). (E) Immunoblot analysis of CST4 protein expression in BT549 vector (Vec) and CST4- overexpressed cells. (F, G) Anchorage-independent growth of BT549 Vec and CST4-overexpressed cells (n=3; *, $p<0.01$). Scale bar = 25 μm.

Supplementary Files

This is a list of supplementary files associated with this preprint. Click to download.

- SupplementalFigures20220801.pdf
- SupplementalTable1.pdf
- Supplementalfullblots.pdf
- Supplementallegends20220804.pdf